http://dx.doi.org/10.21577/0103-5053.20160261

J. Braz. Chem. Soc., Vol. 28, No. 6, 1063-1073, 2017.
Printed in Brazil - ©2017 Sociedade Brasileira de Química
0103 - 5053 $6.00+0.00

Article

Synthesis, Characterization and Dielectric Properties of New 5-(4-Hydroxyphenyl)-10,15,20-tri-4-[2-(3-pentadecylphenoxy)ethoxy]phenyl porphyrin and Their Ni, Co and Cu Complexes

João P. F. Mota,[*,a] Antônio E. da Costa Júnior,[a] Viviane G. P. Ribeiro,[a] Samuel G. Sampaio,[a] Nayane M. A. Lima,[a] Fernando L. F. da Silva,[a] Claudenilson S. Clemente,[a] Giuseppe Mele,[b] Diego Lomonaco[a] and Selma E. Mazzetto[a]*

[a]*Laboratório de Produtos e Tecnologia em Processos (LPT), Departamento de Química Orgânica e Inorgânica, Universidade Federal do Ceará, Campus do Pici, 60440-900 Fortaleza-CE, Brazil*

[b]*Department of Engineering for Innovation, University of Salento, Lecce, Italy*

New asymmetric cardanol-based porphyrins, free-base and coordinated with Ni, Co and Cu, were synthesized and completely characterized as A3B type. Such porphyrins were obtained aiming improved solubility in polar solvents due insertion of an –OH phenolic group. Their thermal and dielectric properties were also evaluated. Changes in the synthetic route reduced the reaction time and improved the yields of the aldehyde precursor obtainment. Electronic absorption spectra of the new porphyrins in CH_2Cl_2, EtOH and acetone, indicated a decrease in the ε (molar absorptivity) values with increasing solvent polarity, except for the nickel complex which, in acetone, showed a slight increase of 2% in the ε value. The dielectric measurements showed that the conductivity (σ) and the loss tangent (tan δ) increased with frequency, but the permittivity (ε') decreased. The results showed that the coordination of the porphyrin promoted a significant change in thermal and dielectric properties, specially for to the Ni-complex compound, which presented the best dielectric properties with interesting values of permittivity and loss tangent at 100 MHz (19.46 and 0.011 a.u., respectively).

Keywords: asymmetric porphyrins, cardanol, dielectric properties

Introduction

Porphyrins are relatively planar aromatic system consisting of four pyrrole type rings joined by four methynic carbons. They have attracted scientists from many areas due to their biological importance, their fascinating physical, chemical, and spectroscopic properties.[1] These compounds have a high electron density due to its 18 π-electrons delocalized on the macrocyclic ring, which are responsible for their spectroscopic characteristics.[2] Porphyrin and its derivatives play multiple roles in nature, such as energy transfer and light absorption in a wide range of the electromagnetic spectrum. Such features are of great interest to the industry of optoelectronic components, such as solar cells, due to its ability to act as photosensitizers when irradiated under visible light.[3] Thus, this is certainly one of the most promising areas of application for these compounds. The structural modeling and synthesis of new porphyrins has grown exponentially in order to control their electronic and thermal properties.[4] The addition of substituents at the *meso* positions and metal ions in the center of porphyrins can improve the electrical and magnetic properties, protecting against auto-oxidation and reducing the formation of dimers. However, these structural modifications can promote, in some cases, a significant decrease in their planarity.[5]

A simple way to obtain porphyrins is the acid catalyzed condensation reaction of pyrrole with specific aldehyde, followed by oxidation of the porphyrinogen. This procedure, originally developed by Rothemund,[6] has been refined by Adler-Longo,[7-9] due to the addition of metal salts to the reaction. Despite the modest yields, the relative simplicity of this method has become suited for preparation of large amounts of tetraarylporphyrins. Higher yields and milder reaction conditions using Lewis acid (TFA or BF_3) as catalyst were obtained by Lindsey *et al.*[10] More recently, substituted asymmetrical porphyrins (A3B, A2B2, etc.) were obtained via mixed

*e-mail: jpfmota@yahoo.com.br

aldehyde condensations, using a mixture of two different aldehydes as starting materials.[11-13]

Asymmetric porphyrins are molecules that exhibit some advantages over the symmetric porphyrins (A4) like: reduced aggregation, groups that allows the use of a wide range of solvents, and presence of dipole moment, which may facilitate the electron injection into the TiO_2 conduction band.[14] In addition, asymmetric porphyrins have been synthesized seeking a better efficacy in photodynamic therapy (PDT), since the cellular affinity depends on amphiphilic character, that is, dependent on the structural arrangement of groups hydrophilic (phenolic –OH or carboxylic –COOH) and hydrophobic (alkyl or aryl chains) *meso*-substituents in macrocycle.[15,16]

Some studies mention the synthesis of porphyrins using cardanol as starting material,[17-19] which provides interesting lipophilic properties, besides being a substance derived from a renewable raw material, the cashew nut shell liquid (CNSL).[20] Cardanol is a phenolic lipid and the main constituent of the CNSL, a dark oil obtained as a by product from industrial processing of the cashew nut (*Anacardium occidentale* L.).[21] It is known that the presence of an alkyl chain or an aryl substituents in porphyrins are important, not just for increase solubility in organic solvents and influence the aggregation of these materials, but also to modify its chemical characteristics and photophysical properties.[11] Here, we report the synthesis and characterization of novel asymmetric cardanol-based A3B porphyrins **4a**-**d** (**4a**: metal-free, **4b**: Ni, **4c**: Co, **4d**: Cu) as well as the study of their thermal and dielectric properties. Scheme 1 shows the steps and reagents used in the preparation of asymmetric porphyrins.

From the thermogravimetric analysis (TGA) it was possible to determine that the thermal stabilities of the porphyrins **4a**-**d**, in inert atmosphere, was in the following order: **4a** > **4d** > **4c** > **4b**. In TGA, the porphyrin **4a** showed initial temperature of degradation at 352 °C (T_{onset}) and other parameters as the final and the half decomposition temperature (T_{endset} and T^*, respectively), the residual mass and the numbers of degradation stages were also evaluated.[22] The dielectric properties, like the loss tangent (tan δ), permittivity (ε') and conductivity (σ) are the most important parameters to determine the suitability for electronics applications.[23,24] According to Lukichev,[25] materials presenting high dielectric constant associated with low loss tangent have important applications in microelectronics. The measurements showed that **4b** have good dielectric permittivity (ca. 20 a.u.) and **4d** had the lowest permittivity (ca. 6 a.u.). These results suggest that the metal promoted a significant change in thermal and electrical properties of the asymmetric porphyrin.

Results and Discussion

Synthesis

The synthesis of porphyrins starting from cardanol are mentioned by many papers since 2004,[26-29] and they employed a procedure which consists in producing an aldehyde derivative as precursor. Normally, this precursor is compound **3** (4-[2-(3-pentadecylphenoxy) ethoxy] benzaldehyde), obtained by a reaction between compound **2** (1-(2-bromoethoxy)-3-pentadecylbenzene) and 4-hydroxybenzaldehyde in acetone using anhydrous potassium carbonate (K_2CO_3) as base, stirred for 24 h and with 40% yield.

In this study, it was found that the replacement of the base, K_2CO_3, by KOH, promoted a decrease on the yield (about 25%), that can be associated with the deprotonation of acetone present in the reaction as solvent.[30] A new reaction procedure using DMF as solvent and KOH as base at 100 °C, provided a better yield (62%) of compound **3** in

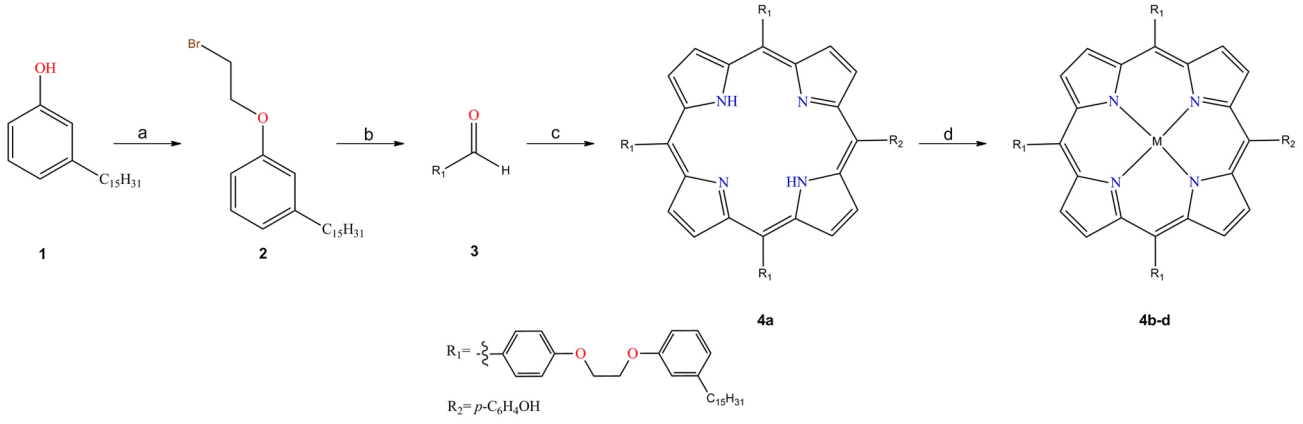

Scheme 1. Synthesis of asymmetric porphyrin **4a** A3B type from cardanol, where (a) KOH, dibromoethane, 70 °C, 6 hours; (b) KOH, DMF, 100 °C, 6 hours; (c) 4-hydroxybenzaldehyde, $CHCl_3$, BF_3, DDQ, 1 hour; (d) acetate metal salts (Ni, **4b**; Co, **4c**; and Cu, **4d**), chloroform/DMF, 3 hours, 90 °C.

only 6 hours of reaction. Based on the result of this new procedure, it is possible to conclude that the DMF is not affected by a strong base.

Characterization

The chemical structures of the asymmetric porphyrin **4a** and its metal complexes **4b**-**d** (A3B type) were characterized using ^{1}H and ^{13}C nuclear magnetic resonance (NMR), matrix-assisted laser desorption ionization-time of flight mass spectrometry (MALDI-TOF-MS), elemental analysis, UV-visible absorption, Fourier transform infrared (FTIR) and fluorescence emission spectroscopy. The FTIR data are listed in Table 1, which were consistent with the proposed structures of the corresponding compounds. For compound **4a**, the absorption bands at 3319 and 967 cm^{-1} are assigned to the N–H stretching and in plane bending vibrations of the pyrrole group, respectively.[2] These absorption bands disappeared in the spectra of metal complexes (**4b**-**d**), since the hydrogen atom of the N–H bond is replaced by a metal ion to form N–M bond, and a new metal-sensitive absorption band appeared at ca. 1000 cm^{-1}, which further confirmed the formation of metal complexes.[31] Moreover, the presence of aliphatic groups in porphyrins **4a**-**d**, are also evident by the presence of absorbance peaks at 2923 and 2852 cm^{-1}, which are characteristic of asymmetric and symmetric νC–H modes, respectively.[17] In addition, the compounds exhibit absorption bands of the phenyl groups at ca. 1610 cm^{-1}, assigned to the C=C stretching vibration.[32]

Table 1. FTIR data to asymmetric porphyrins and its vibrations mode in cm^{-1} (KBr)

4a	4b	4c	4d	Vibration mode
3319	–	–	–	νN–H
2923	2923	2923	2923	νC–H (Ar)
2852	2852	2852	2852	νC–H (Ali)
1607	1608	1608	1608	νC–C (Ar)
1349	1353	1351	1345	νC–N
1245	1246	1246	1245	νAr–O–C
967	–	–	–	δ N–H
	1004	1001	999	N–M

The ^{1}H NMR and ^{13}C NMR spectra were in accordance with the assigned structures and presented all the expected signals for asymmetrical *meso*-substituted porphyrins derived from cardanol. The signals obtained in $CDCl_3$ (^{1}H NMR, Figure 1) for **4a**-**d** exhibited the spectral signatures of the porphyrin core and signals typical of the peripheral cardanol units, such as the singlet at 1.26 ppm corresponding to the 72 protons of the aliphatic groups (–CH_2–).

For free base porphyrin **4a**, the characteristic chemical shift of pyrrole N–H located into the porphyrin ring is located at −2.73 ppm. If we assume equivalence 1 for the peak at 8.84 ppm which was assigned to 8H (β-pyrrolic), the integration of the other peaks can be related to the following hydrogens: peak at 4.48-4.54 ppm to 12H (O–$(CH_2)_2$–O), at 2.64 ppm to 6H (Ph–CH_2), at 0.88 ppm to 9H (CH_3) and peak at 5.29 ppm to 1H (Ph–OH). These peaks indicated that the porphyrin 4a is an asymmetric compound of A3B type. After formation of complexes (**4b**-**d**), the signal peak at −2.73 ppm disappeared, since the hydrogen atom in the N–H bond is replaced by a metal ion.[33] In some paramagnetic metalloporphyrins the signals may be broad due to the hyperfine electron-nuclear interactions and by relaxation processes.[11] Figure 1 shows that compounds **4c** (cobalt porphyrin) and **4d** (copper porphyrin) presented this phenomenon, thus indicating the paramagnetic character of these metals. ^{13}C NMR data to **4a** showed signals that confirm the presence of alkyl (13.85-35.83 ppm), ethers (66.22 ppm) and aromatic groups (111.37-158.45 ppm). Similar signals were observed for metalloporphyrins **4b**-**d** (Figure S1). The results indicated that compounds **4a**-**d** were obtained with good purity, which was confirmed by mass spectrometry (MALDI-TOF, Figure S2) and elemental analysis. The *m/z* for the molecular ion presented the following values: 1669.938 (**4a**), 1726.860 (**4b**), 1726.907 (**4c**) and 1731.889 (**4d**).

Electronic absorption and luminescence spectra

Electronic absorption spectra of porphyrins **4a**-**d** in CH_2Cl_2, EtOH and acetone (Figure 2), show one intense band in the near-ultraviolet region of the spectrum (Soret or B band) and absorption bands at higher wavelengths in the visible region (Q bands). The free base porphyrin **4a** have four Q bands denoted as IV, III, II, and I,[32] while the metallated porphyrins presented one (**4b** and **4c**) or two Q bands (**4d**) due to the increase of symmetry of the complexes.[34] Characteristic Q and B (Soret) bands of metalloporphyrins are determined by transitions of the π-electrons between two higher occupied and two lower unoccupied orbitals.[35] Nevertheless, the changes in the molecular structure and the effect of the solvent may alter the spectra of the porphyrins.[36] The molar absorptivity coefficient values (ε) of Soret band of the porphyrins **4a**-**d** are shown in Table 2, and the results indicated a decrease in the values of ε with increasing solvent polarity, except for the nickel porphyrin (**4b**), in which there was a slight increase of 2% at the ε obtained in acetone. The low values of the molar absorptivity coefficient (Table 2) of the compounds in ethanol clearly indicate the formation of

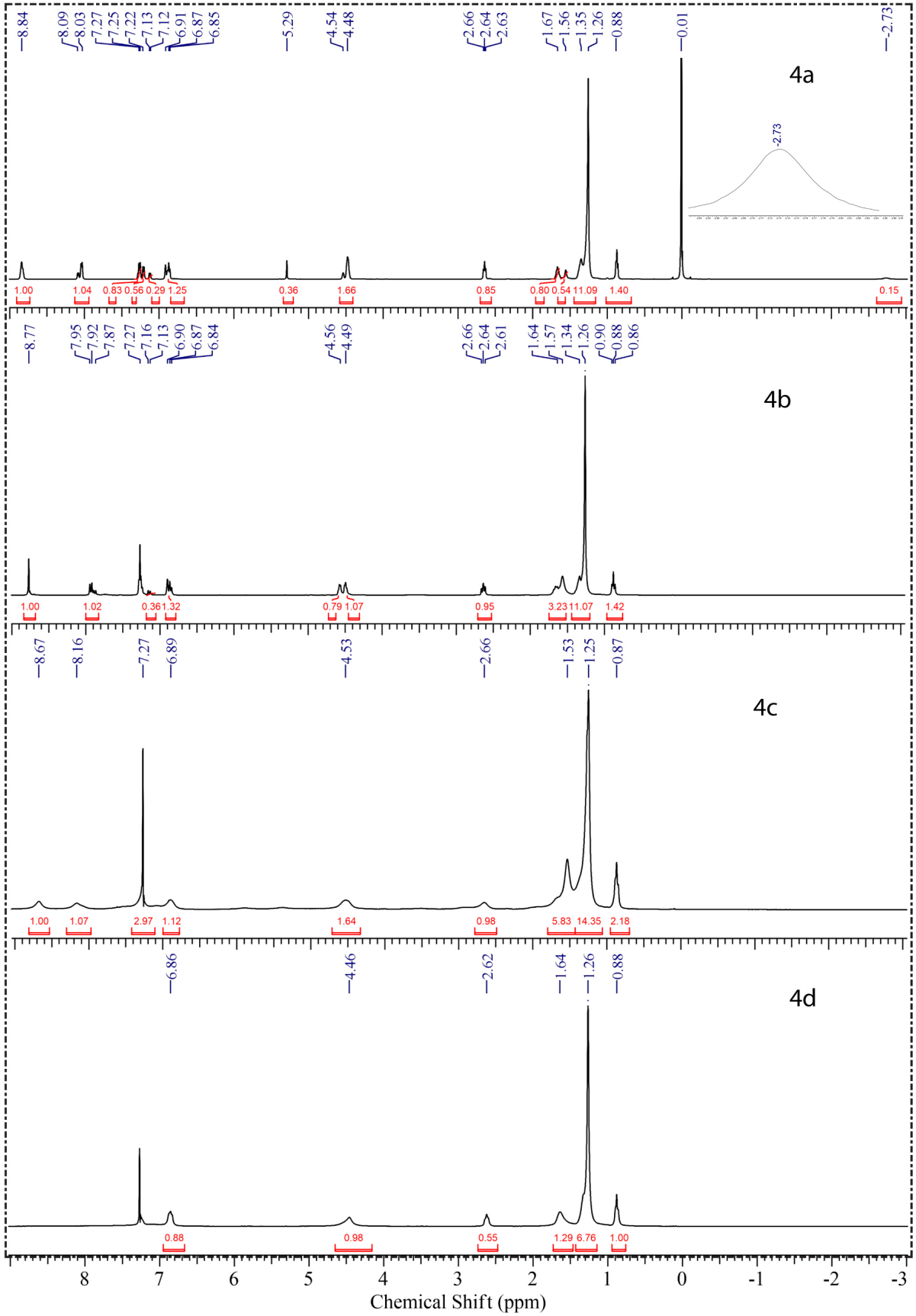

Figure 1. ^{1}H NMR (300 MHz, $CDCl_3$) of asymmetric porphyrins **4a**-**d**.

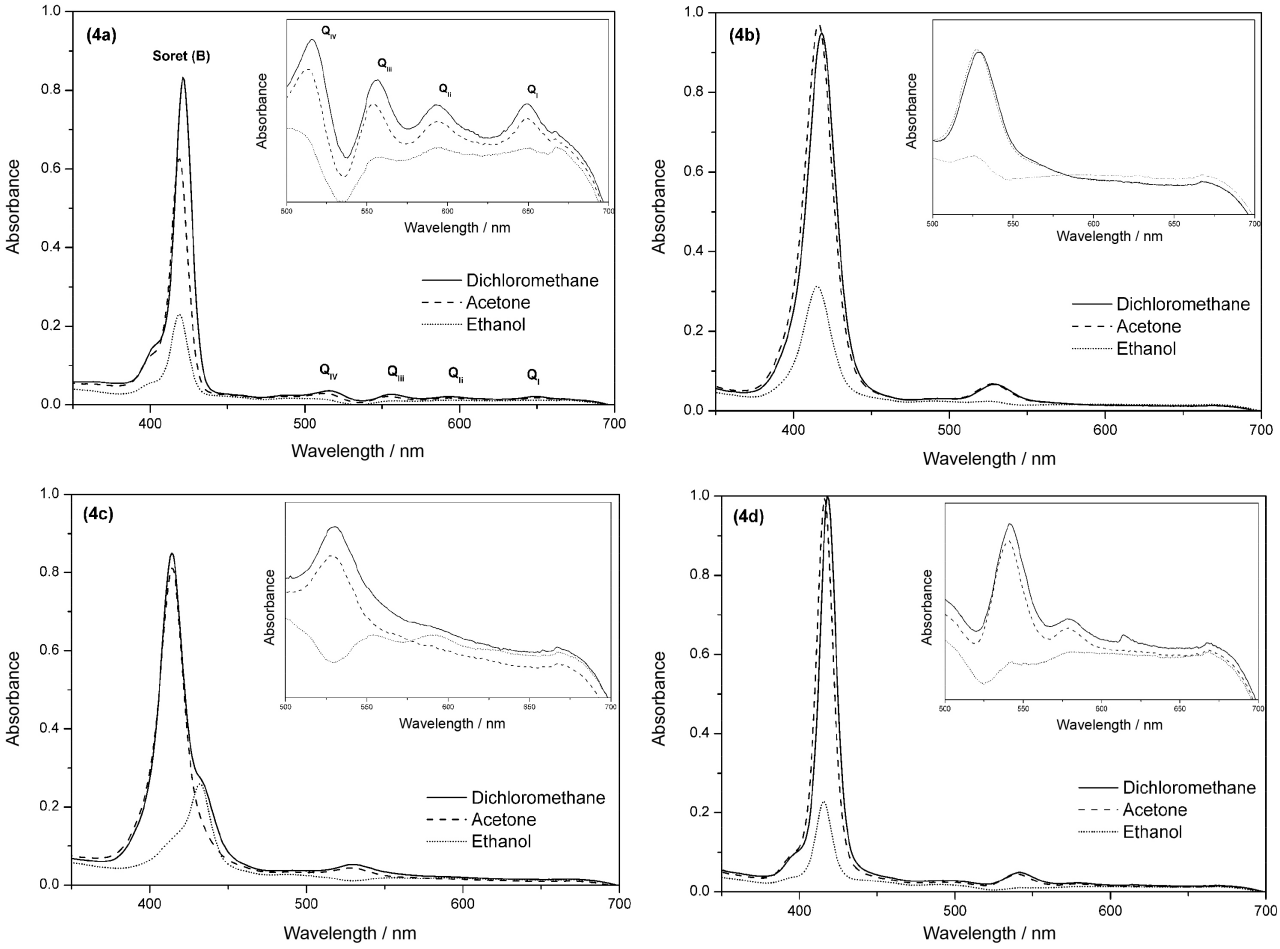

Figure 2. Electronic absorption spectra of porphyrins **4a**-**d**, in the following concentrations: **4a** 1.5 × 10^{-6} M; **4b** 8.0 × 10^{-6} M; **4c** 8.0 × 10^{-6} M and **4d** 2.5 × 10^{-6} M.

Table 2. Molar absorptivity coefficient (ε) of asymmetric porphyrins **4a**-**d** in different organic solvents at 25 °C

Sample	Dichloromethane		Acetone		Ethanol	
	λ_{max} / nm	ε / (10^5 L mol^{-1} cm^{-1})	λ_{max} / nm	ε / (10^5 L mol^{-1} cm^{-1})	λ_{max} / nm	ε / (10^5 L mol^{-1} cm^{-1})
4a	421	5.542	418	4.170	419	1.523
4b	417	1.181	416	1.215	415	0.391
4c	414	1.060	414	1.012	432	0.325
4d	418	3.986	415	3.965	415	0.909

aggregated species, due to, probably, the poor solubility in this solvent, evidenced by decrease in the intensity of the absorption bands (hypochromic effect).

Specifically for compound **4c**, we observe the formation of J-aggregates that showed a red-shifted absorption band at 432 nm.[37] This phenomenon indicated that the molecules of compound **4c** have side-by-side interactions in an ethanolic solution. Usually, porphyrins derived from cardanol have good solubility in solvents with low polarity such as chloroform (μ = 1.04), dichloromethane (μ = 1.60) and THF (μ = 1.75), but they are insoluble in polar solvents like acetone (μ = 2.88). Therefore, these asymmetric porphyrins **4a-d** allowed us to work with a greater variety of solvents, including acetone. This significant change on the solubility of these porphyrins probably occurs due to the presence of the hydroxyl group at the macrocyclic structure, which promotes a better interaction and affinity to polar solvents.

Fluorescence emission spectroscopy of porphyrin **4a** and metalloporphyrins **4b**, **4c** and **4d** were investigated in dichloromethane (10^{-5} M) at room temperature. The emission spectrum of the porphyrin **4a** showed two bands in the red region, one intense at 658 nm (ca. 5 × 10^7) and a lower one at 715 nm (ca. 1 × 10^7) after excitation at 421 nm

(Figure 3A). This spectral behavior was similar to other *meso*-porphyrins and indicates that these compounds can be used in optoelectronic systems working in the red spectral region, for example as catalyst, solar cells, OLEDs (organic light-emitting diode) and photodynamic therapy.[38,39] The fluorescence emission was attributed to the transition from the excited singlet state S_1/S_2 to the ground state S_0 ($S_2 \rightarrow S_0$, $S_1 \rightarrow S_0$). The spectra of the complexes **4b-d** showed a very weak fluorescence band, and when **4b** is excited at 421 nm, this band appeared at 651 nm with intensity about 2×10^3 a.u. (Figure 3B). The decrease in the emission band intensity to porphyrins **4b**-**d** probably occurred due to the heavy atom effect, where the presence of atoms with higher atomic numbers increases the probability of non-radiative transitions.[40,41] The excitation spectrum of **4a** (Figure 4) showed bands responsible for emission with major wavelength at 658 nm. Comparing the excitation spectrum with the absorption spectrum is possible to observe that the emission happened from the absorption of the Soret and Q bands.

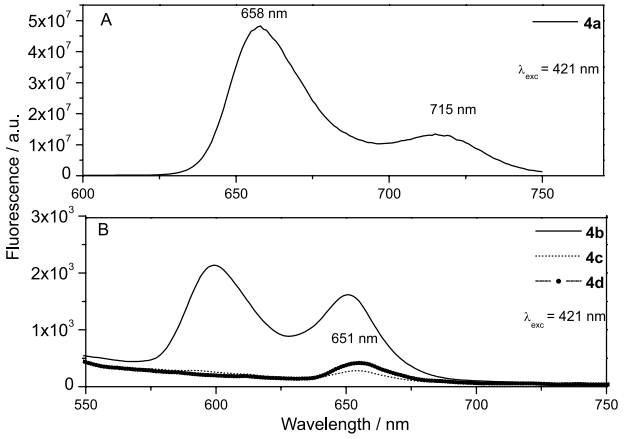

Figure 3. Fluorescence emission spectra of the free base porphyrin **4a** (A) and the complex **4b**, **4c** and **4d** (B) with a concentration of 10^{-5} M in CH_2Cl_2.

Thermal stability

In order to evaluate the thermal stability of the compounds **4a**-**d**, TGA studies were carried out in inert atmosphere (N_2) using a temperature range between 25 and 900 °C. In general, the results showed that the order of observed thermal stabilities of the porphyrins **4a**-**d** were: **4a** > **4d** > **4c** > **4b**. Thus, we verified that porphyrin **4a** has the best thermal properties, probably due to the absence of metal coordinated to the center of the macrocycle, that can act as promoter of degradation process. Table 3 summarizes the decomposition range and maximum temperature values, as well as the weight loss of the main stages of degradation and the residual weight. The decomposition of the compounds **4a**, **4c** and **4d** occurred in two different stages, while the porphyrin **4b** presented three stages.

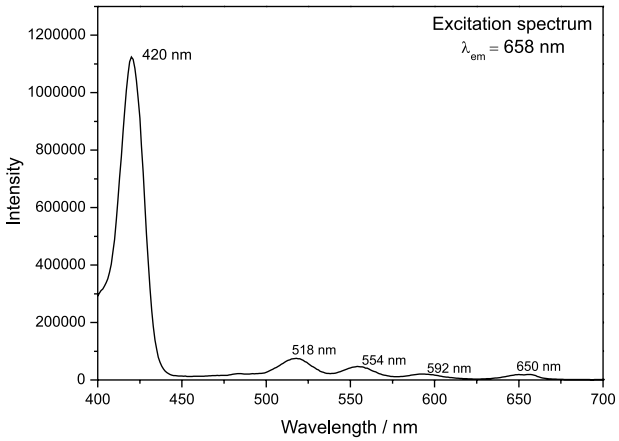

Figure 4. Excitation spectrum of the porphyrin **4a** with emission band in 658 nm.

The first stage of degradation was attributed to the loss of the peripheral chains of cardanol attached to the macrocyclic ring of the porphyrins and the second was associated to the degradation of the macrocycle ring **4a**-**d**.[2] Metalloporphyrins showed initial temperature of degradation lower than the free asymmetric porphyrin **4a**. Similar results was reported by Antina *et al.*,[42] which related the decrease in thermal stability of porphyrins to changes in the aromaticity and π-polarization of the macrocyclic system, due to the presence of the metal ion. Clemente *et al.*[17] showed that the thermal degradation of the symmetric porphyrin, derived from cardanol, started at 250 °C (T_{onset}). This information indicated

Table 3. Thermogravimetric parameters of the two first stages of degradation in N_2 atmosphere

Sample	First stage			Second stage			
	Range temperature / °C	Tmax / °C	Weight loss / %	Range temperature / °C	Tmax / °C	Weight loss / %	Residue / %
4a	352-468	434	64.13	468-702	640	34.19	1.68
4b	161-342	300	46.24	342-477	454	29.25	4.24
4c	166-454	428	50.16	454-581	520	47.11	2.73
4d	328-477	451	49.39	477-658	586	40.09	10.52

that the asymmetric porphyrin **4a** is more thermally stable than its symmetric porphyrin analogue, due to the thermal decomposition of **4a** started only at 352 °C. Therefore, these porphyrins are suitable for applications in technological areas that require luminescent compounds (red region) and elevated thermal stability, like OLEDs and solar cells.[43] During the second stage of thermal degradation, all samples showed gradual mass loss between 29.25 and 47.11% in the temperature range of 342 to 702 °C.

Dielectric properties

Dielectric permittivity (ε') is a measure that shows the ability of materials to store energy and have their dipoles oriented when subjected to an alternating electric field. This capacity is associated with the electric susceptibility of these compounds. The extent of the polarization is directly related to the nature of the material, shape and their structures. Therefore, if the electrical properties (dielectric permittivity) are known, it is possible to predict the influence of an electric field in the polarization of the material studied.

The dielectric permittivity and dielectric loss tangent (tan δ) of porphyrins **4a**-**d** were obtained at room temperature using the following relationship:[44,45]

$$Z = 1 / iw\varepsilon C_0 = 1 / iw(\varepsilon' + i\varepsilon'')C_0 \quad (1)$$

where ε' and ε'' are the real (permittivity) and imaginary parts (dielectric loss) of the dielectric function, respectively. C_0 ($C_0 = \varepsilon_0 A / d$) is the empty cell capacitance, where, A is the electrode area, d is the thickness sample, ε_0 is the permittivity of free space ($\varepsilon_0 = 8.854 \times 10^{-12}$ F m^{-1}) and w ($w = 2\pi f$) is the angular frequency. The components of the complex dielectric function was derived using the relations,

$$\varepsilon' = C / C_0 \text{ and } \varepsilon'' = -i\sigma / wC \quad (2)$$

where C is the capacitance and σ is the conductivity. The imaginary part of the dielectric function can be calculated as $\varepsilon'' = \varepsilon' \tan\delta$. This expression determines the dielectric loss.

It was observed a small decrease in the dielectric permittivity for all asymmetric porphyrins (**4a**-**d**), when the applied frequency was increased (Figure 5). At frequencies greater than 1 MHz it was observed that the values practically did not change. The values of dielectric permittivity at low frequencies can be assigned to different types of polarization, such as dipole or electronic.[42] According to the data, it was observed that this slight decrease in dielectric permittivity resulted from the decrease in polarization of the molecules across electric field. When comparing the dielectric permittivity values of the analyzed molecules, we can see that the porphyrin **4b** had the highest permittivity (ca. 20 a.u.), while **4d** porphyrin had the lowest (ca. 6 a.u.). These results indicated that the compound **4b** is more susceptible to polarization, since higher permittivity values are resulted from the dipole generation. The decrease in the dielectric permittivity value with increasing frequency can be attributed to dipole relaxation phenomenon in which the dipoles at low frequencies follow the frequency of the applied field.[46] However, with the increase frequency, the oscillations in the dipoles cannot follow the applied field and tend to disappear due to the limited time for its polarization.[47]

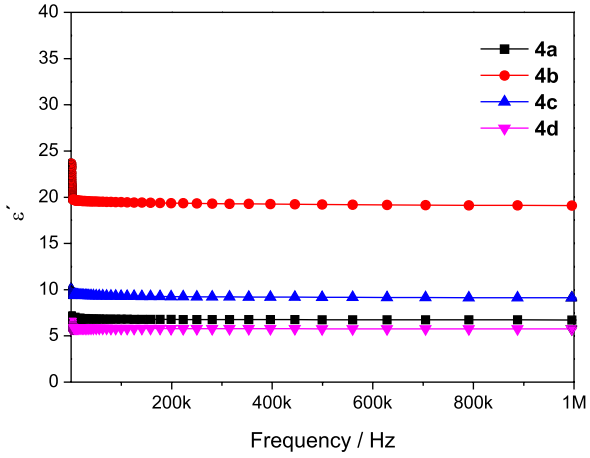

Figure 5. Dielectric permittivity with frequency to porphyrins **4a**-**d** at room temperature.

Dielectric loss tangent is characterized by the loss of energy due to the movement and orientation of electric dipoles of the material, where compounds that have low dielectric loss are considered suitable for use in microelectronics.[48] The dielectric loss tangent (tan δ, Figure 6) was determined as a function of frequency and the results obtained for compounds **4a**-**d** indicated that this parameter increases proportionally with the frequency. In general, the compounds showed low loss tangent and exhibited dispersion for high values in ca. 100 kHz. Porphyrin **4b** showed the best dielectric characteristics, since it combines a high value of dielectric permittivity (19.46 at 100 kHz) and a low dielectric loss tangent (0.011 at 100 kHz).

The results in Table 4 shows that when a metal ion was added in the center of asymmetric porphyrin, the dielectric properties were significantly altered.[23] The increase in the dielectric permittivity (ε') of the **4b** porphyrin (about three times), compared with the free porphyrin **4a** (permittivity

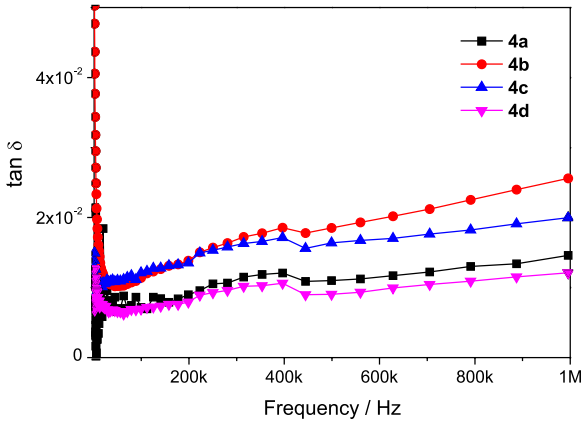

Figure 6. Frequency dependence of the dielectric loss tangent at room temperature.

6.96), is a proof of this influence. Another important parameter of the dielectric properties is the conductivity (σ), and it is associated with migration of charge carriers.[49] The conductivity in alternating current (σ_{ac}) of the asymmetric porphyrins at room temperature was determined as described by Deger *et al.*[50] The porphyrin coordinated with nickel (**4b**) had the highest conductivity values at all frequencies: 1.3×10^{-8} Sm^{-1} (1 kHz), 2.8×10^{-8} Sm^{-1} (10 kHz), 1.9×10^{-7} Sm^{-1} (100 kHz) and 4.6×10^{-6} Sm^{-1} (1 MHz). For other porphyrins, the maximum conductivities were observed in 1 MHz to **4a** (8.6×10^{-7} Sm^{-1}), **4c** (1.6×10^{-6} Sm^{-1}) and **4d** (6.7×10^{-7} Sm^{-1}), respectively. These conductivities indicated that the compounds studied have low polarization when subjected to an external electric field.

Conclusions

The novel metal-free porphyrin **4a** and their metallated analogs **4b**-**d**, were successfully synthesized and characterized like asymmetric porphyrins A3B type. The results of TGA/DTA (differential thermal analysis) analysis showed that the metalloporphyrins have lower initial temperature of degradation (**4b**, **4c** and **4d**) compared to free asymmetric porphyrin (**4a**). The dielectric measurements indicates that the asymmetric porphyrins **4b** have good dielectric properties, due to its better dielectric permittivity and low loss tangent. This study indicates that the coordination of the porphyrin nucleus with a metal promoted a significant change in thermal and electrical properties of these compounds.

Experimental

Reagents

All the starting reagents used in this work were purchased from Sigma-Aldrich Chemical, Vetec, Dynamics, Synth and Acros Organic, and used as received. Solvents were previously distilled before their use.

Analyses

UV-Vis: analyses were performed on a Varian Cary 5000 spectrophotometer, where the spectrum was obtained using quartz cells of 1.0 cm optical path ($CHCl_3$) in the following concentration: **4a** 1.5×10^{-6} M, **4b** 8.0×10^{-6} M, **4c** 8.0×10^{-6} M and **4d** 2.5×10^{-6} M. FTIR: spectra were obtained using a PerkinElmer Spectrum One spectrophotometer, and the samples were prepared as pellets (KBr). ^1H NMR and ^{13}C NMR: was obtained in a nuclear magnetic resonance Bruker Avance DPX 300 spectrometer, operating at 300 (^1H) and 75 MHz (^{13}C) ($CDCl_3$). TGA/DTA: the thermal stability of the samples was evaluated by thermogravimetric analysis It was used an equipment Mettler Toledo TGA/SDTA 851e. The decomposition analyses were performed under nitrogen atmosphere in a constant flow of 50 mL min^{-1}, with heating rate of 10.0 °C min^{-1}, sample mass of 5.0 mg and a temperature program from 25 to 900 °C. MS: samples were analyzed on a Bruker Microflex LT (MaldiTof) using alphacyano, and dichloromethane as a matrix and 5% TFA as mobile phase. Elemental analysis (CNH): the percentual composition of the samples was analyzed on a PerkinElmer 2400 Series II. Dielectric measurements: the samples were shaped in a cylinder, with metal bases (Al). They were pressed by two electrodes connected in order to perform capacitance measurements, dielectric loss, impedance real and imaginary. Measurements were made at room

Table 4. Values of the dielectric properties to asymmetric porphyrins at room temperature

Compound	1 kHz		10 kHz		100 kHz		1 MHz	
	ε'	tan δ	ε'	tan δ	ε'	tan δ	ε'	tan δ
4a	6.96	0.007	6.87	0.003	6.80	0.007	6.73	0.015
4b	20.36	0.073	19.66	0.016	19.46	0.011	19.10	0.026
4c	9.65	0.014	9.43	0.011	9.30	0.012	9.12	0.020
4d	5.97	0.008	5.86	0.008	5.81	0.007	5.75	0.012

temperature in atmospheric air through a precision Agilent 4294A impedance analyzer connected to a microcomputer in the 1 Hz-10 MHz frequency range.

Synthesis of the asymmetric porphyrins

Cardanol precursors of the porphyrins

Hydrogenated cardanol (**1**) was obtained in our laboratory through chromatographic separation of the constituents of CNSL followed by hydrogenation.[51] The compound 1-(2-bromoethoxy)-3-pentadecylbenzene (**2**) derived from **1**, was prepared and characterized by FTIR, and ^{1}H NMR according to the procedure previously described.[52]

Aldehyde (**3**)

Compound 4-[2-(3-pentadecylphenoxy)ethoxy] benzaldehyde (**3**) was obtained by a mix of **2** (3.0 g, 7.30 mmol) and 4-hydroxybenzaldehyde (1.3 g, 10.90 mmol) using KOH (1.3 g, 23.30 mmol) as base in 50 mL of DMF. The system was maintained in stirring at 100 °C for 6 h, and the progress of reaction was carried out by thin layer chromatography (TLC). The reaction mixture was subjected to a pretreatment by means of a liquid-liquid partition with distilled water (200 mL) and ethyl acetate (200 mL). The organic phase was dried with anhydrous Na_2SO_4, concentrated and purified in column chromatography with silica gel having as eluent hexane/ethyl acetate (95:5). The compound **3** was obtained in 62% yield (2.0 g), molecular weight 452.67 g mol^{-1} ($C_{30}H_{44}O_3$).

Metal-free porphyrin (**4a**)

The free base 5-(4-hydroxyphenyl)-10,15,20-tri-4-[2-(3-pentadecylphenoxy)ethoxy]phenyl porphyrin (**4a**) was obtained by a mix of the pyrrole (0.88 mmol), **3** (0.88 mmol), 4-hydroxybenzaldehyde (0.22 mmol), NaCl (16.25 mmol), BF_3 (0.22 mmol) and DDQ (0.50 mmol) in chloroform/ethanol (50 mL, ethanol 0.8%) at room temperature for 1 hour. The crude was packaged in a silica column chromatography and eluted with solvents of increasing polarity: dichloromethane, dichloromethane/ethanol (9:1). The asymmetric free base porphyrins (**4a**) were obtained in the second fraction eluted and the compound was recrystallized with ethanol/hexane. **4a**: yield 26%. ^{1}H NMR (300 MHz, $CDCl_3$) δ –2.73 (s, 2H, N–H), 0.88 (t, 9H, *J* 6.5 Hz, CH_3), 1.26 (s, 72H, CH_2–$(CH_2)_{12}$–CH_3), 1.67 (m, 6H, Ph–CH_2–CH_2), 2.64 (t, 6H, *J* 8.0 Hz, Ph–CH_2), 4.52 (d, 12H, *J* 4.5 Hz, O–$(CH_2)_2$–O), 5.29 (s, 1H, Ph–OH), 6.85-8.09 (28H, Ph–H), 8.84 (s, 8H, H-β pyrrolic); ^{13}C NMR (75 MHz, $CDCl_3$) δ 13.85 (CH_3), 22.42 (CH_2–CH_3), 29.43-31.66 (CH_2–$(CH_2)_{13}$–CH_3), 35.83 (Ph–CH_2), 66.22 (O–$(CH_2)_2$–O), 111.37-158.45 (C-aromatic); FTIR (KBr) ν / cm^{-1} 3436, 3319, 2923, 2852, 1607, 1583, 1509, 1448, 1245, 1158, 1071, 967; UV-Vis (CH_2Cl_2) λ_{max} / nm 421, 516, 557, 592, 649; MS (MALDI-TOF) *m/z*, for $C_{113}H_{144}N_4O_7$ [M$^+$], observed: 1669.938; required: 1670.375; elemental analysis (CNH) for $C_{113}H_{144}N_4O_7$, observed: C 81.29, N 3.65, H 8.76%; required: C 81.25, N 3.35, H 8.69%.

Metalloporphyrins (**4b-d**)

4a (0.06 mmol) and acetate metal salts (0.60 mmol, Ni, **4b**; Co, **4c**; and Cu, **4d**) were added in a mix of the chloroform/DMF (20 mL of each) for 3 hours at 90 °C. The product was purified by chromatography in a silica gel column using dichloromethane as eluent, and the product collected in the first fraction eluted corresponding to compounds **4b**-**d**. The metalloporphyrins were recrystallized with a mix of ethanol/hexane.

4b

Yield 89%. ^{1}H NMR (300 MHz, $CDCl_3$) δ 0.88 (t, 9H, *J* 6.3 Hz, CH_3), 1.26 (s, 72H, CH_2–$(CH_2)_{12}$–CH_3), 1.64 (m, 6H, Ph–CH_2–CH_2), 2.64 (t, 6H, *J* 7.5 Hz, Ph–CH_2), 4.55 (d, 12H, *J* 4.8 Hz, O–$(CH_2)_2$–O), 6.84-7.95 (28H, Ph–H), 8.77 (s, 8H, H-β pyrrolic); ^{13}C NMR (75 MHz, $CDCl_3$) δ 14.08 (CH_3), 22.66 (CH_2–CH_3), 29.36-31.90 (CH_2–$(CH_2)_{13}$–CH_3), 36.06 (Ph–CH_2), 66.88 (O–$(CH_2)_2$–O), 111.67-158.73 (C-aromatic); FTIR (KBr) ν / cm^{-1} 3432, 2923, 2852, 1608, 1584, 1507, 1448, 1246, 1158, 1074, 1004; UV-Vis (CH_2Cl_2) λ_{max} / nm 416, 529; MS (MALDI-TOF) *m/z*, for $C_{113}H_{142}N_4O_7Ni$ [M$^+$], observed: 1726.860; required: 1727.054; elemental analysis (CNH) for $C_{113}H_{142}N_4O_7Ni$, observed: C 79.56, N 2.21, H 9.38%; required: C 78.59, N 3.24, H 8.29%.

4c

Yield 79%. ^{1}H NMR (300 MHz, $CDCl_3$) δ 0.87 (t, 9H, *J* 5.4 Hz, CH_3), 1.25 (s, 72H, CH_2–$(CH_2)_{12}$–CH_3), 1.53 (broad signal, 6H, Ph–CH_2–CH_2), 2.66 (broad signal, 6H, Ph–CH_2), 4.53 (broad signal, 12H, O–$(CH_2)_2$–O), 6.89-8.16 (broad signals, 28H, Ph–H), 8.67 (broad signal, 8H, H-β pyrrolic); ^{13}C NMR (75 MHz, $CDCl_3$) δ 13.69 (CH_3), 22.27 (CH_2–CH_3), 28.96-31.51 (CH_2–$(CH_2)_{13}$–CH_3), 35.78 (Ph–CH_2), 67.41 (O–$(CH_2)_2$–O), 111.48-158.44 (C-aromatic); FTIR (KBr) ν / cm^{-1} 3436, 2923, 2852, 1608, 1583, 1507, 1449, 1246, 1158, 1073, 1001; UV-Vis ($CHCl_3$) λ_{max} / nm 414, 530; MS (MALDI-TOF) *m/z*, for $C_{113}H_{142}N_4O_7Co$ [M$^+$], observed: 1726.907; [M$^+$] required: 1727.298; elemental analysis (CNH) for $C_{113}H_{142}N_4O_7Co$, observed: C 77.77, N 3.39, H 8.45%; required: C 78.57, N 3.24, H 8.29%.

4d

Yield 83%. ^{1}H NMR (300 MHz, $CDCl_3$) δ 0.88 (t, 9H, *J* 6.0 Hz, CH_3), 1.26 (s, 72H, CH_2–$(CH_2)_{12}$–CH_3), 1.64 (broad signal, 6H, Ph–CH_2–CH_2), 2.62 (broad signal, 6H, Ph–CH_2), 4.46 (broad signal, 12H, O–$(CH_2)_2$–O), 6.86 (broad signal, 6H, H-aromatic); ^{13}C NMR (75 MHz, $CDCl_3$) δ 14.10 (CH_3), 22.66 (CH_2–CH_3), 29.36-31.89 (CH_2–$(CH_2)_{12}$–CH_2), 36.07 (Ph–CH_2), 66.45 (O–$(CH_2)_2$–O), 111.61-158.70 (C-aromatic); FTIR (KBr) ν / cm^{-1} 3434, 2923, 2852, 1608, 1583, 1504, 1447, 1245, 1158, 1072, 999; UV-Vis ($CHCl_3$) λ_{max} / nm 418, 542, 578; MS (MALDI-TOF) *m/z*, for $C_{113}H_{142}N_4O_7Cu$ [M$^+$], observed: 1731.889; required: 1731.896; elemental analysis (CNH) for $C_{113}H_{142}N_4O_7Cu$, observed: C 78.28, N 3.47, H 8.41%; required: C 78.37, N 3.23, H 8.26%.

Supplementary Information

Supplementary information is available free of charge at http://jbcs.org.br as PDF file.

Acknowledgments

The authors would like to thank the support from CAPES and CNPq (PVE 401359/2014-0 and 402566/2013-0), Almonds Company in Brazil by providing cashew nuts, CENAUREMN (Centro Nordestino de Aplicação e Uso da Ressonância Magnética Nuclear, Brazil) for the NMR analyses

References

1. Birin, K. P.; Gorbunova, Y. G.; Tsivadze, A. Y.; Bessmertnykh-Lemeune, A. G.; Guilard, R.; *Eur. J. Org. Chem*. **2015**, *25*, 5610.
2. Sun, E.; Shi, Y.; Zhang, P.; Zhou, M.; Zhang, Y.; Tang, X.; Shi, T.; *J. Mol. Struct.* **2008**, *889*, 28.
3. Li, K.; Lin, L.; Peng, T.; Guo, Y.; Li, R.; Zhang, J.; *Chem. Commun*. **2015**, *51*, 12443.
4. Henriques, C. A.; Gonçalves, N. P. F.; Abreu, A. R.; Calvete, M. J. F.; Pereira, M. M.; *J. Porphyrins Phthalocyanines* **2012**, *16*, 290.
5. Basova, T. V.; Çamur, M.; Esenpinar, A. A.; Tuncel, S.; Hassan, A.; Alexeyev, A.; Banimuslem, H.; Durmus, M.; Gurek, A. G.; Ahsen, V.; *Synth. Met*. **2012**, *162*, 735.
6. Rothemund, P.; *J. Am. Chem. Soc*. **1935**, *57*, 2010.
7. Adler, A. D.; Longo, F. R.; Shergalis, W.; *J. Org. Chem*. **1964**, *86*, 3145.
8. Adler, A. D.; Longo, F. R.; Finarelli, J. D.; Godmacher, J.; Assour, J.; Korsakoff, L.; *J. Org. Chem*. **1967**, *32*, 476.
9. Adler, A. D.; Sklar, L.; Longo, F. R.; Finarelli, J. D.; Finarelli, M. G.; *J. Heterocycl. Chem*. **1968**, *5*, 669.
10. Lindsey, J. S.; Schreiman, I. C.; Hsu, H. C.; Kearney, P. C.; Marguerettaz, A. N.; *J. Org. Chem.* **1987**, *52*, 827.
11. Guo, Y.-C.; Xiao, W.; Mele, G.; Martina, F.; Margapoti, E.; Mazzetto, S. E.; Vasapollo, G.; *J. Porphyrins Phthalocyanines* **2006**, *10*, 1071.
12. Zhuang, C.; Tang, X.; Wang, D.; Xia, A.; Lian, W.; Shi, Y.; Shi, T.; *J. Serb. Chem. Soc*. **2009**, *74*, 1097.
13. Schiavon, M. A.; Iwamoto, L. S.; Ferreira, A. G.; Iamamoto, Y.; Zanoni, M. V. B.; Assis, M. D.; *J. Braz. Chem. Soc*. **2000**, *11*, 458.
14. Urbani, M.; Gratzel, M.; Nazeeruddin, M. K.; Torres, T.; *Chem. Rev*. **2014**, *114*, 12330.
15. Fagadar-Cosma, E.; Cseh, L.; Badea, V.; Fagadar-Cosma, G.; Vlascici, D.; *Comb. Chem. High Throughput Screening* **2007**, *10*, 466.
16. Peng, C.-L.; Lai, P.-S.; Shieh, M.-J.; *Biomed. Eng.-App. Bas. C.* **2008**, *20*, 9.
17. Clemente, C. S.; Ribeiro, V. G. P.; Sousa, J. E. A.; Maia, F. J. N.; Barreto, A. C. H.; Andrade, N. F.; Denardin, J. C.; Mele, G.; Carbone, L.; Mazzetto, S. E.; Fechine, P. B. A.; *J. Nano Res*. **2013**, *15*, 1739.
18. Sandrino, B.; Clemente, S. C.; Oliveira, T. M. B. F.; Ribeiro, F. W. P.; Pavinatto, F. J.; Mazzetto, S. E.; Neto, P. L.; Correia, N. A.; Pessoa, C. A.; Wohnrath, K.; *Colloids Surf., A* **2013**, *425*, 68.
19. Bloise, E.; Carbone, L.; Colafemmina, G.; D'Accolti, L.; Mazzetto, S. E.; Vasapollo, G.; Mele, G.; *Molecules* **2012**, *17*, 12252.
20. Attanasi, O. A.; Mele, G.; Filippone, P.; Mazzetto, S. E.; Vasapollo, G.; *Arkivoc* **2009**, *viii*, 69.
21. Júnior, A. E. C.; Barreto, A. C. H.; Rosa, B. S.; Maia, F. J. N.; Lomonaco, D.; Mazzetto, S. E.; *J. Compos. Mater*. **2015**, *49*, 2203.
22. Guan, C.; Li, L.; Chen, D.; Gao, Z.; Sun, W.; *Thermochim. Acta* **2004**, *413*, 31.
23. Saleh, A. M.; Hraibat, S. M.; Kitaneh, R. M.-L.; Abu-Samreh, M. M.; Musameh, S. M.; *J. Semicond.* **2012**, *33*, 082002-1.
24. Canlıca, M.; Altındal, A.; Nyokong, T.; *J. Porphyrins Phthalocyanines* **2012**, *16*, 826.
25. Lukichev, A. A.; *Chem. Phys.* **2014**, *428*, 29.
26. Mele, G.; Vasapollo, G.; *Mini-Rev. Org. Chem.* **2008**, *5*, 243.
27. Mele, G.; Del Sole, R.; Vasapollo, G.; Garcia-Lopez, E.; Palmisano, L.; Mazzetto, S. E.; Attanasi, O. A.; Filippone, P.; *Green Chem*. **2004**, *6*, 604.
28. Vasapollo, G.; Mele, G.; Del Sole, R.; Pio, I.; Li, J.; Mazzetto, S. E.; *Molecules* **2011**, *16*, 5769.
29. Vasapollo, G.; Mele, G.; Del Sole, R.; *Molecules* **2011**, *16*, 6871.
30. Clayden, J.; Greeves, N.; Warren, S.; Wothers, P.; *Organic Chemistry*; Oxford University Press: Oxford, USA, 2001 (with corrections in 2009), p. 690.

31. Xu, Z.; Mei, Q.; Hua Q.; Tian, R.; Weng, J.; Shi, Y.; Huang, W.; *J. Mol. Struct.* **2015**, *1094*, 1.
32. Yu, M.; Chen, G.-J.; Liu, G.-F.; *J. Phys. Chem. Sol.* **2007**, *68*, 541.
33. Brem, B.; Gal, E.; Gaina, L.; Cristea, C.; Gabudean, A. M.; Astilean, S.; Silaghi-Dumitresco, L.; *Dyes Pigments* **2015**, *123*, 386.
34. Yu, M.; Zhang, Y. J.; Shi, J. H.; Liu, G. F.; Zhang, H. J.; *Solid State Sci.* **2009**, *11*, 2016.
35. Wei, L.; TongShun, S.; *Sci. China, Ser. B: Chem*. **2007**, *50*, 488.
36. Sun, E.-J.; Sun, Z.-Y.; Yuan, M.; Wang, D.; Shi, T.-S.; *Dyes Pigments* **2009**, *81*, 124.
37. Fagadar-cosma, E.; Vlascici, D.; Fagadar-cosma, G.; Palade, A.; Lascu, A.; Creanga, I.; Birdeanu, M.; Cristescu, R.; Cernica, I.; *Molecules* **2014**, *19*, 21239.
38. Valicsek, Z.; Horváth, O.; *Microchem. J.* **2013**, *107*, 47.
39. Zheng, W.; Shan, N.; Yu, L.; Wang, X.; *Dyes Pigments* **2008**, *77*, 153.
40. Borisevich, E. A.; Solov'ev, K. N.; *Phys.-Usp.* **2005**, *48*, 231.
41. Nastasi, F.; Campagna, S.; Ngo, T. H.; Dehaen, W.; Maes, W.; Kruk, M.; *Photochem. Photobiol. Sci*. **2011**, *10*, 143.
42. Antina, E. V.; Balantseva, E. V.; Berezin, M. B.; *Russ. J. Gen. Chem.* **2011**, *81*, 1222.
43. Chevrier, M.; Kesters, J.; Blayo, C.; Richeter, S.; Van Der Lee, A.; Coulembier, O.; Surin, M.; Mehdi, A.; Lazzaroni, R.; Evans, R. C.; Maes, W.; Dubois, P.; Clément, S.; *Macromol. Chem. Phys*. **2016**, *217*, 445.
44. Yazici, A.; Ünüs, N.; Altindal, A.; Salih, B.; Bekaroglu, O.; *Dalton Trans*. **2012**, *41*, 3773.
45. Yang, J.; Yang, X.; Pu, Z.; Chen, L.; Liu, X.; *Mater. Lett.* **2013**, *93*, 199.
46. Yu, L.; Zhang, Y.; Tong, W.; Shang, J.; Lv, F.; Ke, S.; Huang, H.; *Proc. SPIE* **2012**, *8409*, 1.
47. Boonlakhorn, J.; Kidkhunthod, P.; Thongbai, P.; *J. Eur. Ceram. Soc.* **2015**, *35*, 3521.
48. Li, Y.; Yuan, J.; Xue, J.; Cai, F.; Chen, F.; Fu, Q.; *Compos. Sci. Technol.* **2015**, *118*, 198.
49. Zou, Y.; Yang, J.; Zhan, Y.; Yang, X.; Zhong, J.; Zhao, R.; Liu, X.; *J. Appl. Polym. Sci*. **2012**, *125*, 3829.
50. Deger, D.; Ulutaş, K.; Yakut, Ş.; Kara, H.; *Mater. Sci. Semicond. Process.* **2015**, *38*, 1.
51. Lomonaco, D.; Santiago, G. M. P.; Ferreira, Y. S.; Arriaga, A. M. C.; Mazzetto, S. E.; Mele, G.; Vasapollo, G.; *Green Chem*. **2009**, *11*, 31.
52. Attanasi, O. A.; Del Sole, R.; Filippone, P.; Mazzetto, S. E.; Mele, G.; Vasapollo, G.; *J. Porphyrins Phthalocyanines* **2004**, *8*, 1276.

Submitted: June 6, 2016
Published online: September 26, 2016